

# A Query-Driven Dynamic Vision Sensor with Spatiotemporal Filtering

Daniel Weiss\*, Kameron Gano\*, Audrey Meador\*, Gabby Fortuno\*, Eric Cito\* Solana Fernandez\*

\*equal contribution; Jacobs School of Engineering, University of California, San Diego, La Jolla, CA, 92092

**Abstract**—The proposed query-driven dynamic vision sensor (qDVS) advances the state-of-the-art in low-power vision sensing by incorporating spatiotemporal filtering to enhance image quality by reducing detectable noise. While existing qDVS designs significantly reduce energy consumption, they do little to reduce potential noise. By spatially filtering photocurrent across neighboring pixels and temporally filtering across sequentially detected and instantaneously experienced changes, image noise is reduced. This results in a more desirable image that still costs little power to detect.

**Index Terms**—Query-Driven, Dynamic Vision Sensing, Neuromorphic Computing

## I. INTRODUCTION

In general, query-driven dynamic vision sensing (qDVS) offers lower power consumption compared to active pixel sensing (APS) or traditional event-driven dynamic vision sensing (eDVS). APS pixels indiscriminately report at each time frame, whereas event-driven dynamic vision sensing (eDVS) pixel only outputs a response when there is a significant shift in brightness. By integrating the advantages of both APS and eDVS, we achieve qDVS, which employs clocked time-division multiplexing to periodically scan the array and detect threshold changes in pixel intensity. Based on Kubendran's work [1], this fast and ultra-low-power periodic scanning is controlled by three external clocks that drive gray counters. These counters generate address codes to navigate through the rows and columns, enabling the readout of pixel event data. The row decoder sequentially selects one row at a time, allowing all columns to be queried simultaneously.

The present gold-standard qDVS technology by PROPHESEE/Sony presents exceptional pixel size ( $4.86\mu\text{m} \times 4.86\mu\text{m}$ ) and fill factor (77%) [2] when compared to CelePixel ( $9.8\mu\text{m} \times 9.8\mu\text{m}$ , 8%) [3], Samsung ( $9\mu\text{m} \times 9\mu\text{m}$ , 11%) [4], IniLabs ( $31.2\mu\text{m} \times 31.2\mu\text{m}$ , 10.3%) [5], and Y. Chi et al. using delta difference sampling (DDS) ( $25.3\mu\text{m} \times 25.2\mu\text{m}$ , 17%) [6], where fill factor is defined as the fraction of the detector element area that is active in light detection. Furthermore, it offers an energy efficiency of 137 pJ/pixel-event [2], whereas the newly proposed approach from Kubendran [1] reduces this value over twenty-fold to 6.34 pJ/pixel-event, while offering the second-best pixel sizing ( $7.6\mu\text{m} \times 7.6\mu\text{m}$ ) and fill factor (33%). This type of vision sensor utilizes temporal filtering, capturing the difference between consecutive intensity measurements, enabling the sensor to filter out sparsity over time, and allowing the sensor to ignore unchanging scenes. However, PROPHESEE's approach may cause noisy images

due to its lack of spatial filtering of the photocurrent. Without the addition of spatial filtering, the appearance of the image will likely be more blurred and not enhance finer details.

Our proposed qDVS will utilize spatiotemporal filtering. In addition to the temporal filtering previously done, we employ spatial filtering to analyze the relationship of a given pixel with respect to its neighbors. Spatial filtering will allow the sensor to determine whether a pixel should register an ON or OFF event based on the summation of its individually induced photocurrent and the photocurrent received from surrounding pixels at a given moment, and thus filtering sparsity in space. The combined spatiotemporal filtering aids in data reduction, as the sensor only detects relevant information, and optimizes the sensor's energy efficiency, as only activated pixels that are queried will detect change.

## II. METHODS

### A. Design

The reference design used for the final pixel design is based on the qDVS scheme outlined in Rajkumar Kubendran's work [1]. The overall operating principle, which was the same in our final design, is to have a row of pixels detect a threshold change in  $V_{IN}$  by querying each row at a fixed rate. This is done by setting the row select signal (RS) to Vdd and setting reset to ground in accordance with a clock.

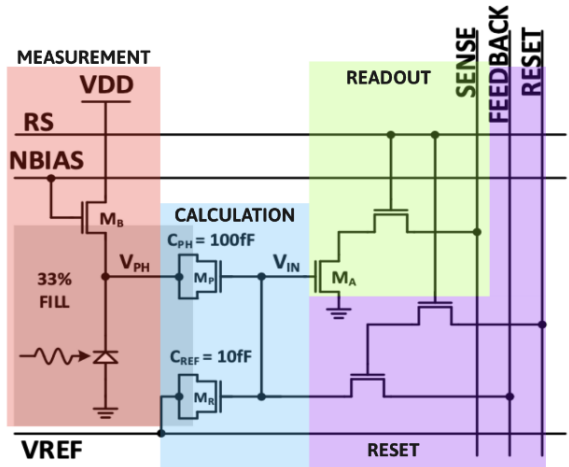


Fig. 1. Reference pixel design given in Rajkumar Kubendran's work [1].

A change in  $V_{IN}$  is a function of  $V_{REF}$  and the log-encoded photo current  $V_{PH}$ . A change in  $V_{IN}$  modulates the current in

the SENSE line which is routed to the periphery of the chip, outlined in a later section. The periphery is responsible for

detecting whether there was a threshold change in  $V_{in}$  indicating an ON or OFF event. This threshold for which a change is detected,  $\epsilon$ , is a parameter of the periphery of the circuit.

$$\Delta V_{in} = \frac{C_{PH}\Delta V_{PH} + C_{REF}\Delta V_{REF}}{C_{PH} + C_{REF}}$$

$$\Delta V_{in} > +\epsilon \Rightarrow \text{ON event}, \quad (1)$$

$$\Delta V_{in} < -\epsilon \Rightarrow \text{OFF event}. \quad (2)$$

The reference voltage  $V_{ref}$  is meant to store the result of the previous measurement. During reset, there is a path from FEEDBACK to  $V_{ref}$ . FEEDBACK is a signal generated at the periphery indicating the measurement state.

The reference pixel design implements temporal filtering by forcing  $V_{ph}$  through a capacitive load, creating a minimum time for which the pixel has to produce a detectable change in photo current. This makes the design inherently robust to temporal sparsity, but there is no mechanism to address spatial sparsity. Sparse spatial activity is a problem for image quality, since it allows for extraneous light to activate pixels that may not be related to the image being detected.

To address this problem in our final design, we make the log-encoded photocurrent  $V_{ph}$  dependent on a pixel's northward, southward, westward, and eastward neighbors. Therefore, the magnitude of a change in  $V_{in}$  for a given change in photocurrent depends on the activity of these four neighbors. For example, if a pixel's four neighbors are all registering to be off and the center pixel receives a change in photocurrent, this change would have to be significant in magnitude in order for the pixel to be able to affect a strong enough change on  $V_{in}$  to register an on event. Overall, this operates as a denoising tactic.

The following formulations exhibit how the log encoded photocurrent  $V_{ph}$  is effected by its neighbors:

#### DECLARATIONS

$$I_{IN} = I_{BIAS} - \beta I_{photo},$$

$$I_{GIORGOS} = I_{WEST} + I_{NORTH} + I_{SOUTH} + I_{EAST} = I_G,$$

$$I_{IN} = I_{GIORGOS}.$$

#### PHOTO DIODE

$$I_{BIAS} = I_0 e^{\frac{K_n V_{gv} - V_{ph}}{V_{th}}} \left( 1 - e^{\frac{-K_n V_{ds}}{V_{th}}} \right).$$

#### FROM KCL

$$e^{\frac{K_n V_{gv} - V_{ph}}{V_{th}}} = \frac{B}{I_0} I_{photo} + I_G,$$

$$K_n V_{gv} - V_{ph} = V_{th} \ln \left( \frac{B}{I_0} I_{photo} + I_G \right),$$

$$V_{ph} = K_n V_{gv} - V_{th} \ln \left( \frac{B}{I_0} I_{photo} + I_G \right),$$

$$= -V_{th} \ln \left( \frac{B}{I_0} I_{photo} + I_G \right) + V_{th} \ln \left( \frac{B}{I_0} I'_{photo} + I_G \right)$$

$$V'_{ph} = V_{ph} - V_{th} \ln \left( \frac{\frac{B}{I_0} I'_{photo} + I_{GIORGOS}}{\frac{B}{I_0} I_{photo} + I_{GIORGOS}} \right)$$

Similarly, it can be shown that there is an exponential decay factor associated with the photo current for an impulse at time  $t=0$  at the center pixel of an infinitely large grid of pixels. This decay factor shows how a change at a single pixel affects neighboring pixels. Solving for this term involves finding the thevenin equivalent conductance in one direction, and then using our assumptions to simplify our analysis:

$$G_{INF} = \frac{-G_v + \sqrt{G_v^2 + 4G_v G_H}}{2}$$

$$I_{in} = I_{out,i} + 4I_{out,i+1} \left( 1 + \frac{G_{INF}}{G_v} \right)$$

$$I_{in,ij} = I_{out,ij} + 4I_{out,i\pm 1,j\pm 1} \left( \frac{G_v + \sqrt{G_v^2 + 4G_v G_H}}{2G_v} \right)$$

where  $G_{inf}$  is the thevenin equivalent conductance as seen by the measurement node of a neighboring pixel, and  $G_v$  and  $G_H$  are the conductances associated with bias voltages  $V_{gv}$  and  $V_{gh}$ , respectively. Because there are four directions for which a pixel can affect a change and our assumption was that this grid of pixels was infinite, the thevenin equivalent conductance in all four directions is the same. Therefore, we can multiply the current seen in the  $(i+1)$ -th pixel by the decay factor.

Moreover, the exponential decay factor depends on conductances  $G_v$  and  $G_H$ , implying that the ratio between the bias voltages  $V_{gv}$  and  $V_{gh}$  directly effect this decay factor.

The two transistors that implement spatial filtering are biased with the voltage  $V_{gv}$ , which provides an effective weighting factor to neighboring pixel connections. This can be increased for a stronger sensitivity to neighboring changes and decreased for a weaker sensitivity to neighboring changes.

#### B. Periphery

The periphery is a critical component in our architecture, responsible for detecting threshold changes in the SENSE line current and encoding these events into a digital signal. Drawing inspiration from Kubendran et al. [1], our periphery design incorporates an inverting amplifier and a voltage clamp to process and stabilize the signal. Fig. 3 shows the connection between the SENSE line, inverting amplifier, voltage clamp, and feedback signal.

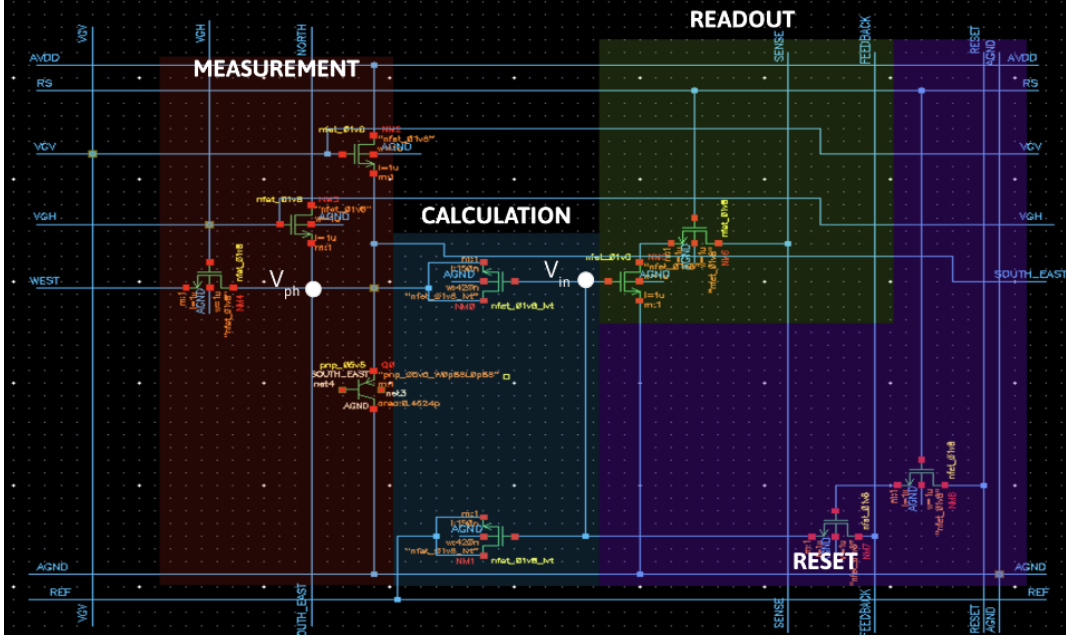


Fig. 2. The final pixel schematic with connections to northward, southward, westward, and eastward connections, implementing spatial filtering.

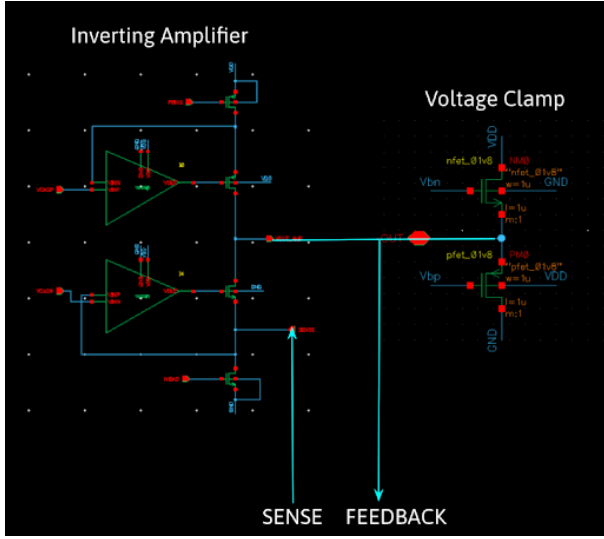


Fig. 3. Schematic of labeled periphery components, inspired from Kubenbранд's work [1].

The inverting amplifier is connected to the SENSE line and serves as the first stage of processing. It translates variations in  $I_{sense}$ , induced by changes in pixel voltage  $V_{in}$ , into a corresponding voltage output. The key function of the amplifier is to detect whether  $I_{sense}$  has surpassed a threshold value, signaling an ON or OFF event. The output on the FEEDBACK line undergoes a high-to-low transition in response to increasing  $I_{sense}$ , digitizing the event information.

To further process the signal, a voltage clamp is connected to the output of the inverting amplifier. The clamp limits the output voltage swing, ensuring that the amplifier operates

within its region of high gain. This stabilization prevents the amplifier from entering non-linear or saturated regions, preserving the sharp transitions in the FEEDBACK signal that are essential for detecting threshold events. Additionally, the voltage clamp ensures that the output remains within a well-defined range, which improves the readability and consistency of the signals for subsequent processing. This design ensures that the periphery processes spatiotemporal changes accurately and maintains robust performance across varying conditions.

To store the results of previous measurements and prepare for the next cycle, the reference voltage  $V_{ref}$  is updated during the reset phase:

- 1) During threshold event detection, a change in  $V_{in}$  causes  $I_{sense}$  to exceed the threshold, prompting a transition in FEEDBACK from ON to OFF.
- 2) In the reset phase, a path is established from FEEDBACK to  $V_{ref}$ , allowing the feedback signal to adjust the reference voltage.
- 3) Then, the reference voltage,  $V_{ref}$ , is updated, reflecting the last detected change in  $V_{in}$ , which ensures that the system adapts dynamically to subsequent input variations.

### C. Single Pixel Layout

We implemented our pixel layout in the Skywater 130nm process using Cadence® Virtuoso® to perform design rule check (DRC) and LVS (layout versus schematic) verification. All seven nMOS transistors are implemented as nfet\_01v8 (with dimensions 1um x 1um), the two nMOS capacitors as nfet\_01v8\_lvt (with dimensions 150nm x 420nm), and Positive-Negative-Positive (PNP) Bipolar Junction Transistor (BJT) as pnP\_05v5 in the core library of the SKY130 PDK.

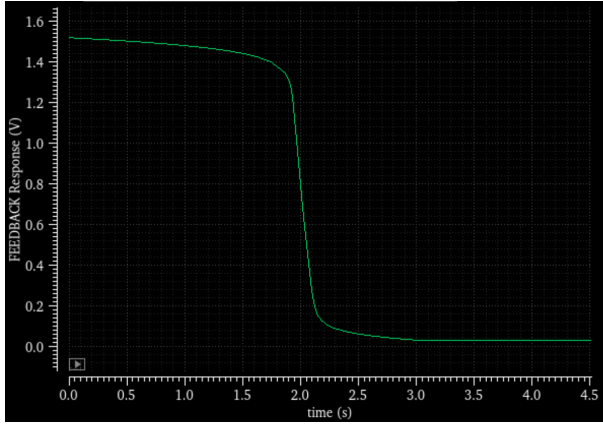


Fig. 4. Feedback Response and Threshold Detection. The FEEDBACK signal generated by the periphery is a direct indication of the measurement state. The FEEDBACK voltage transitions from high to low as  $I_{sense}$  increases beyond the threshold, aligning with the desired behavior for spatiotemporal event detection.

Using a low-threshold n-MOS transistor as a MOSCAP has specific advantages, primarily due to its impact on the operating characteristics and ease of achieving desired capacitance behavior. A low threshold voltage requires less gate voltage to reach saturation, resulting in lower power consumption. When measuring capacitance-voltage characteristics in MOSCAPS, the smooth transition from depletion to inversion is essential. A low-threshold device provides better linearity in these inversion regions, making data interpretation and modeling more straightforward.

Under normal conditions, the n-well of pMOS transistors is connected to the power supply ( $V_{dd}$ ), which keeps the parasitic BJT in a reverse-biased state. In this state, the BJT does not conduct active current, only a reverse diode junction leakage current. Because of this behavior, we ignored the parasitic BJT in circuit analysis and removed it from the extracted netlist. Nonetheless, if the n-well is left floating, photon absorption can generate electron-hole pairs in the base-emitter depletion region of the parasitic BJT, inducing a photocurrent. This light-induced effect forward-biases the junction, amplifying the photocurrent by a large factor (around 50) at the collector. As a result, this parasitic PNP phototransistor structure is often more sensitive to light than a simple photodiode (n-diffusion to p-substrate) and is preferred for detecting very low light levels.

This single pixel design is free from any DRC errors and passes LVS. The measured pixel size is  $8.2\mu\text{m} \times 8.2\mu\text{m}$  with a photosensitive area  $27.2384 \mu\text{m}^2$ , yielding a fill factor of 40.5%, which is greater than Kubendran's qDVS. [1].

### III. RESULTS

#### A. Simulation Setup

In order to test the ability of the pixel design to spatially filter, temporally filter, and sense photocurrent, a 3-by-3 grid of pixels was used in simulation. The photodiode of each pixel was replaced with an ideal current source. The

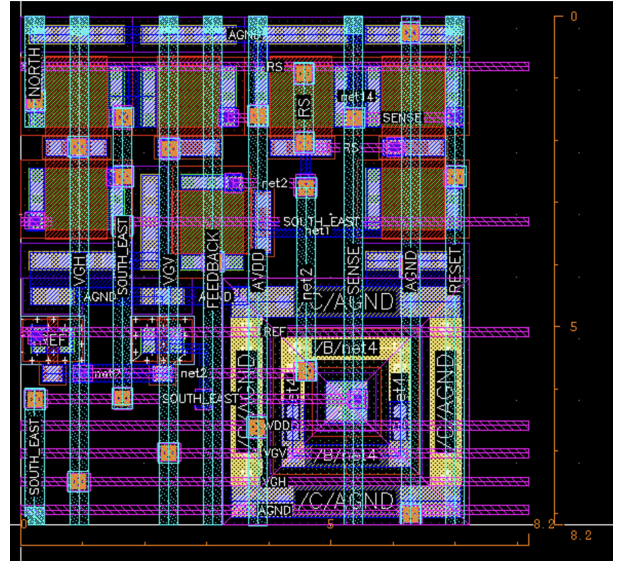


Fig. 5. Physical layout of a single qDVS pixel, with a size of  $8.2\mu\text{m} \times 8.2\mu\text{m}$  and 40.5% fill factor.

outside pixels' photocurrent were undriven and held at 1 nA, simulating a high photocurrent and a bright room. However, the center pixel's photocurrent operated as a piecewise function, cycling between 1 nA for 0.5 s and 1 fA for 0.5 s at 0.5 Hz. A visualization of this setup can be seen in Fig. 6., and a comparison of the driven and undriven photocurrents can be observed in Fig. 7.

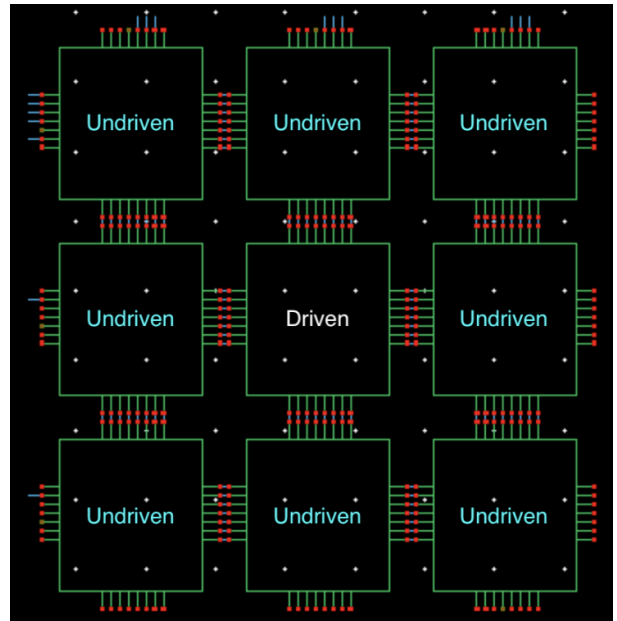


Fig. 6. A 3-by-3 grid of pixels with the center photocurrent being driven.

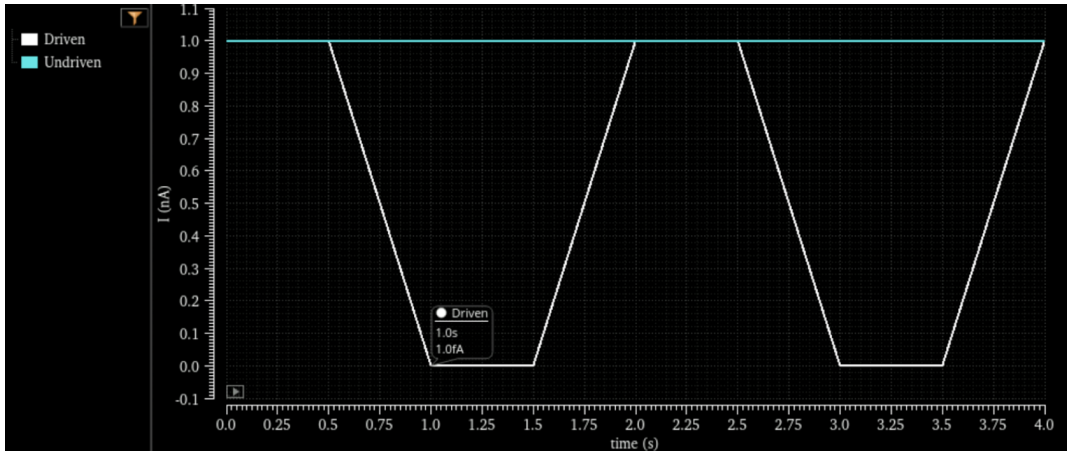


Fig. 7. A comparison of the undriven photocurrent at 1 nA (bright room) vs. the driven photocurrent between 1 nA and 1 fA (cycling between the bright and dark room respectively).

### B. Spatial Filtering

Spatial filtering was verified using the setup above by measuring the voltage at the Vph node in pixels progressively further away from the central, driven one. The voltages at the Vph nodes in each pixel were shared via their North and West connections. As can be observed in Fig. 8., as the photocurrent decreased, the resulting Vph,i of the central pixel rose from 196.2 mV to 207.1 mV. In addition, the Vph of its neighbor, Vph,i+1, and its neighbor's neighbor, Vph,i+2, also rose but to an increasingly lesser degree: 199.3 mV and 198.0 mV respectively. In an infinite grid, the relationship between the voltages at incrementally further pixels would be geometric. This ideal case could not properly be simulated though, so the relationship was not quite geometric. The experimental k factor increased from 0.28 in the first step to 0.58 in the second step because the rim pixels had fewer immediate neighbors to share their Vph with. Regardless, the capacity of the pixel design to spatially filter can be observed in how the voltage increase caused by the changing photocurrent in the central pixel was shared with its neighbors even though the photocurrent at those pixels did not change. Furthermore, the spatial filtering can be tuned by adjusting the Vgv and Vgh bias voltages.

To contrast against the base case, where no spatial filtering is done, the same simulation was run without the North and West connections between the Vph nodes of the pixels in the grid. The results of this test can be seen in Fig. 9. Without the North and West connections between the Vph nodes of the pixels, the increase in voltage caused by the changing photocurrent in the central pixel cannot be shared and is concentrated. As a result, there was a much greater spike in Vph,i at the central pixel. The voltage increased from the baseline of 196.2 mV to 374.7 mV. However, the Vphs of the surrounding pixels remained at 196.2 mV, receiving none of the voltage increase. It is clear the proposed design successfully performed spatial filtering when compared to previous designs.

### C. Temporal Filtering

The temporal filtering is the design is performed by the MOS capacitors and the reset of Vref between detected changes in photocurrent. To begin, the MOS capacitors provide a capacitive load to the circuit. This manifests as a time constant such that a change in Vin is only affected if a change in Vph is observed for a significant amount of time and is not instantaneous. As can be seen in Fig. 10., the relationship between Vph and Vin in the driven pixel is not one-to-one. There were differences in Vin depending on how long Vph held its value for. Furthermore, in Fig. 11., a simulation of a change in photocurrent from 1 nA to 1 fA for a duration of 10 us was performed. Vph spiked from 196.2 mV to 203.9 mV, a 7.8 mV change. In contrast, Vin only spiked from 0 mV to 7.5mV. Given the short duration of the change in photocurrent, Vin was not given enough time to experience the same change that Vph did. As such, a longer exposure to a change in light will affect a larger and more significant change in Vin, and thus a larger and more significant change in current along the Sense wire.

Besides the MOS capacitors, the resetting of Vref performs its own kind of temporal filtering. When Vph/Vin changes enough to enact a threshold change in the current along the Sense wire, the periphery circuit sets the voltage on the reset wire to logic-high. This brings Vref to the voltage on the feedback wire, resetting the Vref baseline. Now, the pixel is ready to detect another threshold change in Sense wire current and has effectively temporally filtered the previously detected change.

### D. Sensing Changes

The remaining question regarding the pixel design is whether it can still detect a meaningful change in photocurrent with the addition of spatial filtering. Two simulations were run to test this. In the first, only the center pixel was driven between 1 nA and 1 fA. The results of this simulation can be seen in Fig. 12. As expected, the middle Sense wire detects a

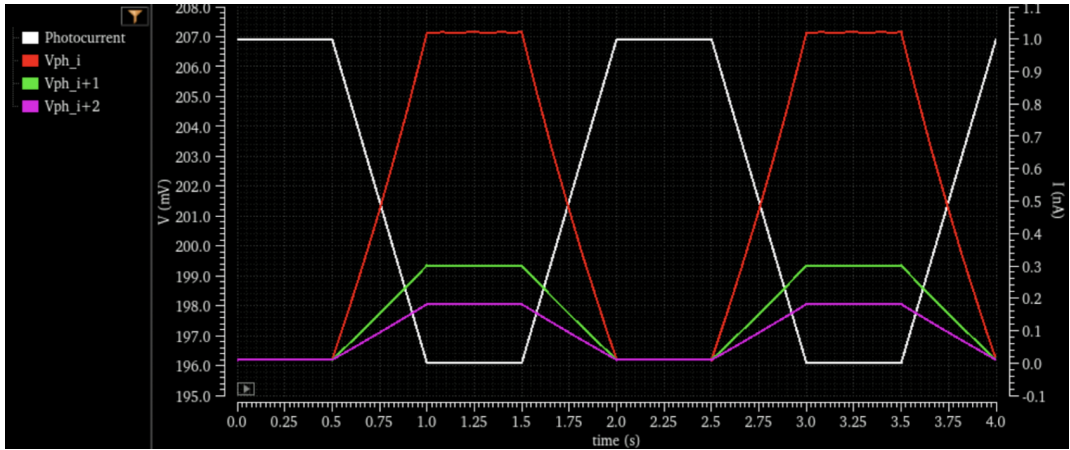


Fig. 8. A comparison of  $V_{ph}$  in pixels incrementally further away from the central, driven one when spatial filtering is used.

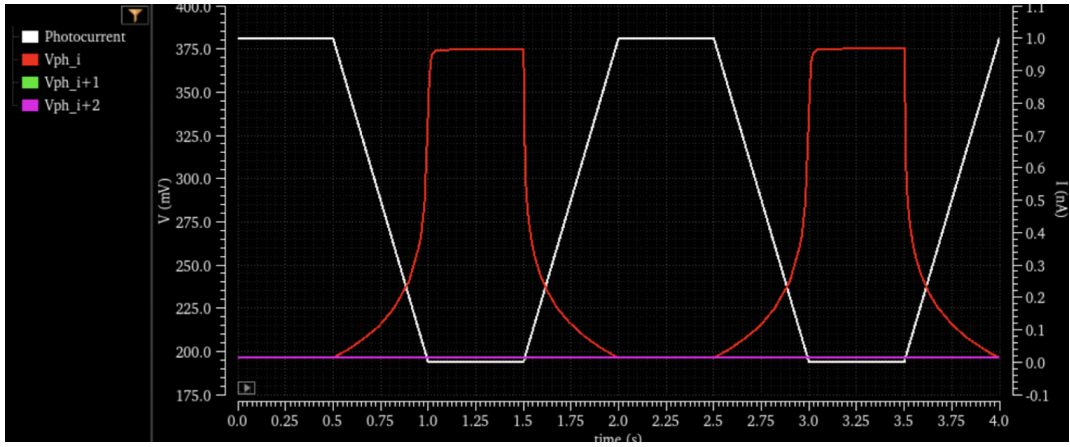


Fig. 9. A comparison of  $V_{ph}$  in pixels incrementally further away from the central, driven one when spatial filtering is not used.

greater change in current than the left or right ones with the left and right Sense wires measuring the same change. Although there is a change in Sense current, it is on the order of 10 fA. This change is not truly detectable, as it is roughly the same magnitude that one might expect leakage current to be. This is expected though, because if only one pixel's photocurrent changes, but none of its neighbors' do, then the change might be noise. Therefore, it is not desirable to detect that change. This is the idea behind the spatial filtering of the pixel.

Conversely, the second simulation tested the scenario where all nine of the pixels experienced the same change in photocurrent between 1 nA and 1 fA. The results of this simulation can be seen in Fig. 13. In the ideal case of an infinite pixel grid, this change in Sense current would be expected to be the same across each column. Here however, the Sense wires detect only roughly the same change. The difference between the Sense currents might be explained by the positioning of the spatial filtering transistor only to the left and top of each  $V_{ph}$  node, and so the edge cases in the 3-by-3 grid cause some inequality. This discrepancy notwithstanding, the changes in photocurrent in this simulation caused changes in Sense current on the order of 1 pA. This is a much more easily detectable and

recognizable change for the periphery circuit. This is expected as well because if a group of pixels all experience the same change in photocurrent, it is less likely to be noise. Therefore, it is desirable to detect those changes, as they pass the spatial filtering. As a result, the pixel design is capable of detecting meaningful change in photocurrent in a pixel grid with spatial filtering.

#### IV. CONCLUSION

This study showed that incorporating spatial filtering into the qDVS design from [1] results in a dependency on the photocurrent log-encoded as  $V_{ph}$ . This innovation has shown promise to reduce noise in image perception through its ability to spatially and temporally filter while still being able to detect meaningful changes in pixel photocurrent.

Spatial filtering is responsible for producing a noise-reduced image by ensuring that isolated pixel activity may or may not register an ON or OFF event depending on the behavior of neighboring pixels. To confirm that neighboring pixels affect each other, an impulse at the center of a 3x3 grid of pixels was simulated. These results demonstrated that when a change was experienced by a single pixel, the surrounding pixels also

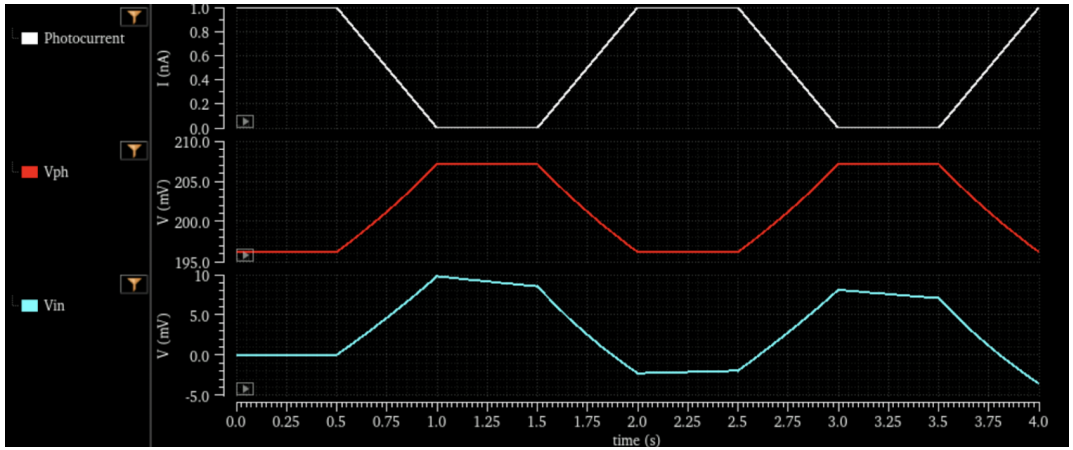


Fig. 10. Relationship between  $V_{ph}$  and  $V_{in}$  at the center pixel as the photocurrent cycled.

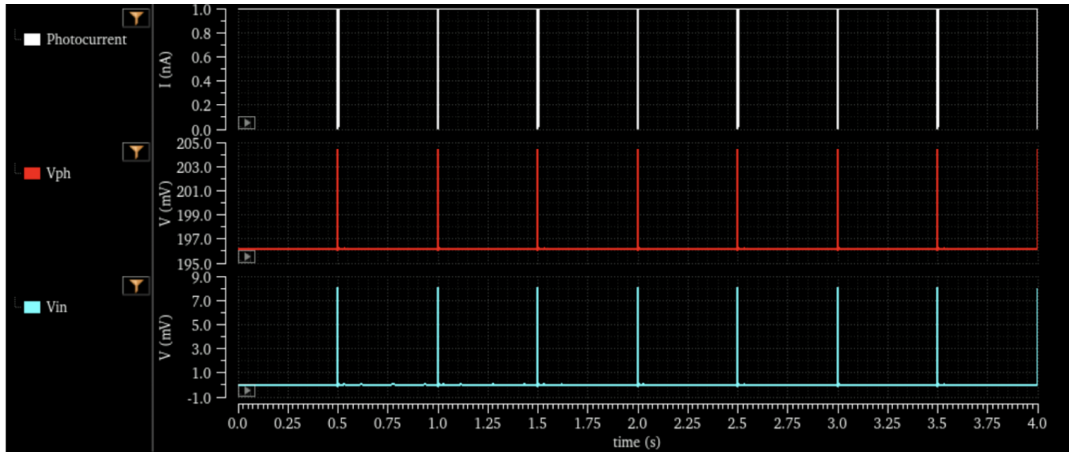


Fig. 11. Relationship between  $V_{ph}$  and  $V_{in}$  at the center pixel given 10  $\mu$ s spikes in photocurrent.

exhibited a change. Specifically, the simulated results indicated that the photocurrent voltage of the driven pixel in the center of a  $3 \times 3$  grid exponentially decays across its surrounding pixels, which is characteristic of spatial filtering. The extent to which spatial filtering has an impact is tunable by adjusting the ratios of  $V_{gv}$  and  $V_{gh}$  as shown in above equations. The ratio of the conductances modulated by these values impacts the percentage of  $V_{ph}$  seen at a neighboring pixel.

Temporal filtering sets a response time for which a change in photocurrent is able to affect a change on  $V_{in}$ . Tying the photodiode to a capacitive load virtually guarantees that discrete impulses of high intensity or low intensity light will not be able to affect a change on  $V_{in}$ . This eliminates the possibility of discrete noise being able to hinder image quality. This was demonstrated by monitoring the behavior of a pixel when both prolonged and near-instantaneous changes in photocurrent were present, and simulation results showed that  $V_{in}$  resisted these changes as desired. A given pixel was much more receptive to longer exposure periods. In addition, the RESET signal enables a new change in photocurrent to be detected, and thus temporally filters from the previously

detected change.

On the other hand, the primary limitation of pixel development and verification was that a photodiode could not be modeled directly in cadence and that we used an ideal current source instead. The efficacy of a photodiode in transducing light to current is process and area dependent, and hands-on testing would need to be done to characterize the sensitivity of the pixel. Also, at the grid level, a critical limitation of our work was that the pixel grid and the periphery were not tested in tandem. This is an issue because the sensitivity of the periphery in detecting a change in SENSE current is bias-dependent. It is not possible to suggest reasonable biases for the periphery of the device without first simulating it with a grid of pixels to characterize the range of current change on the SENSE line. In addition, our simulations were across the whole spectrum of observable photocurrents (1 nA to 1 fA). We have not defined the granularity with which we can resolve a change in the photocurrent that the pixel can detect. This is especially troubling because the spatial filtering can drastically decrease the change in  $V_{ph}$  for a given change in

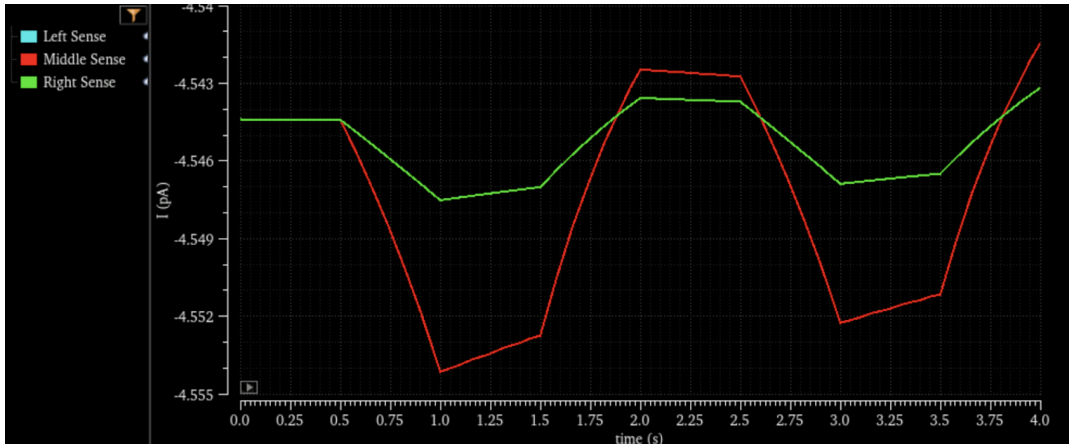


Fig. 12. Detected change in Sense current with only one of nine pixel photocurrents driven.

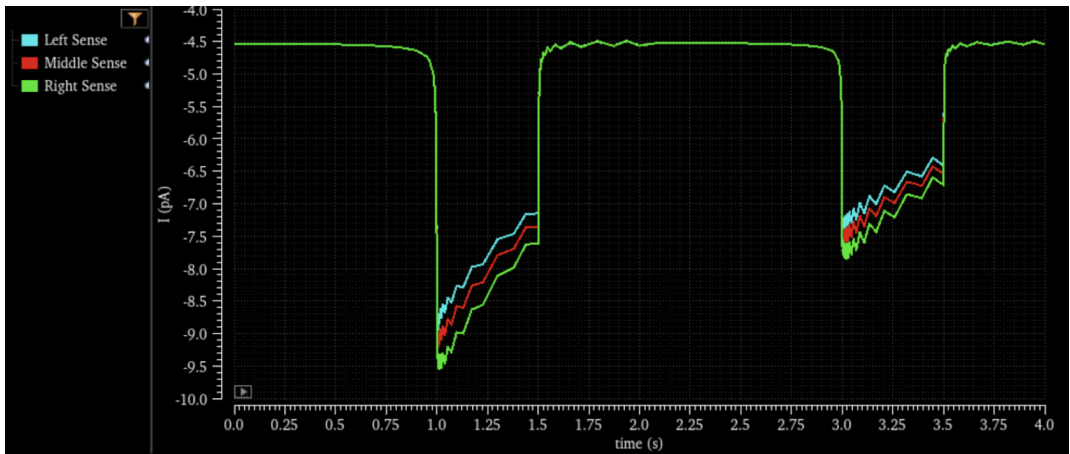


Fig. 13. Detected change in Sense current with all nine pixel photocurrents driven.

photocurrent. We can fine-tune the ratio of  $V_{gh}$  to  $V_{gv}$  in order to help with this, but it adds another thing to consider in fabrication and use.

In future testing, these are areas we will focus on in order to gain a more concrete understanding of the pixel design.

#### ACKNOWLEDGMENTS

Our group would like to thank the effort and support of Dr. Gert Cauwenberghs, Giorgos Gennis, and Shashank Bansal for their unwavering guidance throughout the quarter. The environment the teaching staff fostered was highly conducive to learning and collaboration, and it made what would otherwise be another group project into a formative experience that bonded all of us together. Thank you so much.

#### REFERENCES

- [1] R. Kubendran, A. Paul and G. Cauwenberghs, "A 256x256 6.3pJ/pixel-event Query-driven Dynamic Vision Sensor with Energy-conserving Row-parallel Event Scanning," CICC, 2021
- [2] T. Finateu et al., "A 1280x 720 Back-Illuminated Stacked Temporal Contrast Event-Based Vision Sensor with 4.86  $\mu$ m Pixels, 1.066 GEPS Readout, Programmable Event-Rate Controller and Compressive DataFormatting Pipeline," ISSCC, 2020.

- [3] S. Chen et al., "Live demonstration: CeleX-V: a 1M pixel multi-mode eventbased sensor," CVPRW, 2019.
- [4] S. Bongki et al., "A 640x480 Dynamic Vision Sensor with a 9 $\mu$ m Pixel and 300Meps Address-Event Representation," ISSCC, 2017.
- [5] M. Yang et al., "A Dynamic Vision Sensor With 1% Temporal Contrast Sensitivity and In-Pixel Asynchronous Delta Modulator for Event Encoding," JSSC, 2015.
- [6] Y. Chi et al., "CMOS Camera with In-Pixel Temporal Change Detection and ADC," JSSC, 2007.
- [7] M. Young, *The Technical Writer's Handbook*. Mill Valley, CA: University Science, 1989.